

Complex magnetic ordering in $\text{NdNi}_{1-x}\text{Cu}_x$: Determination of the magnetic structure by neutron diffraction

J. García Soldevilla and J. A. Blanco

Departamento de Física, Universidad de Oviedo, 33007 Oviedo, Spain

J. Rodríguez Fernández, J. I. Espeso, and J. C. Gómez Sal

Departamento de Ciencias de la Tierra y Física de la Materia Condensada, Facultad de Ciencias, Universidad de Cantabria, 39005 Santander, Spain

M. T. Fernandez-Díaz

Institute Max-von Laue-Paul Langevin, F38042 Grenoble Cedex, France

J. Rodríguez-Carvajal

Laboratoire Leon Brillouin, CEA-CNRS, Centre de Etudes de Saclay, 91191 Gif sur Yvette Cedex, France

D. Paccard

Laiman, E.S.I.A., Université de Savoie, BP 240, 74942 Annecy-le-Vieux, France

(Received 28 January 2004; revised manuscript received 8 June 2004; published 13 December 2004)

The magnetic properties of orthorhombic (FeB-type) $\text{NdNi}_{1-x}\text{Cu}_x$ ($x \geq 0.4$) compounds have been studied by measuring magnetic susceptibility, magnetization vs temperature, and applied magnetic field, electrical resistivity, and neutron diffraction on polycrystalline samples. The noncollinear ferromagnetic structure observed for the compositions $0.4 < x < 0.8$, with the magnetic moments within the \mathbf{xz} plane, evolves towards considerably more complex antiferromagnetic orderings characterized by the coexistence of two propagation vectors for the largest Cu content $x=0.9$ and 1.0 , while the intermediate composition $x=0.8$ exhibits a coexistence of ferro- and incommensurate magnetic structures. This magnetic evolution is discussed considering the changes in the distances between Nd—Nd (first and second neighbors) and also the modifications on the density of states at the Fermi level when the Cu content increases.

DOI: 10.1103/PhysRevB.70.224411

PACS number(s): 75.25.+z, 75.30.Cr, 75.30.Kz, 75.60.Ej

I. INTRODUCTION

For more than four decades, intermetallic Rare Earth compounds with nonmagnetic metals have been extensively investigated. Apart from the industrial and technological applications, this field of research is of fundamental interest due to its almost unlimited wealth for the study of basic as well as considerably less conventional topics on magnetism: exchange interactions and their frustration, crystalline electric field coupling, magnetoelastic effects, critical phenomena, etc.¹ For these reasons, these systems are often model ones for making quantitative analyses that lead to an accurate determination of the relevant interactions in play.

In the course of a general study of the physical properties of orthorhombic $\text{RNi}_{1-x}\text{Cu}_x$ compounds (R=Rare Earth) it became clear that structural and electronic effects influence the magnetic properties of these materials.^{2,3} They are particularly sensitive to the balance between both RKKY exchange interactions and crystalline electric field (CEF) effects, showing (i) important modifications on the RKKY interactions driven by the Cu substitutions that lead to a change of magnetic arrangement from ferromagnetism (F) to antiferromagnetism (AF) with an increasing Cu content; (ii) evidence for the existence of a strong magnetocrystalline anisotropy owing to the low local symmetry of the crystallographic $4c$ site occupied by the R^{3+} ion.

In fact, these pseudobinary compounds, where Ni and Cu are both nonmagnetic, crystallize in either the CrB-type (Cmcm space group) or in the FeB-type (Pnma space group) structure for the Ni or Cu rich compositions, respectively.

Most of the studies on these series have previously been performed with heavy Rare Earths while, more recently, a general study has focused on the case of light Rare Earths such as Ce,⁴ Pr,⁵ and Nd.⁶ The cerium-based series behaves as a Kondo system showing a complex magnetic phase diagram with competing interactions and also revealing the existence of a cluster-glass phase.⁷ The $\text{PrNi}_{1-x}\text{Cu}_x$ compounds are simple paramagnetic systems for the Cu rich compositions due to the existence of a singlet ground state well isolated from the other excited levels.⁵ Finally, the $\text{NdNi}_{1-x}\text{Cu}_x$ system provides an excellent field for studying the interplay between strong CEF anisotropy and indirect exchange interactions connecting well localized Nd^{3+} magnetic moments.⁶ This preliminary work revealed that the FeB-type structure holds for Cu concentrations $0.4 \leq x \leq 1.0$, providing a wide range of stability of this phase, and showing that the change from F to AF ordering takes place around $x=0.8$.

It is worth mentioning at this point the complex magnetic structures appearing in pure Nd and some Nd-based compounds; e.g., pure Nd metal is a paradigmatic example of multi- q magnetic structures⁸ and NdCu_2 also presents a squared up magnetic structure, very sensitive to an applied magnetic field.⁹ Furthermore, preliminary work on the mag-

netic structure of NdCu showed two different propagation vectors.¹⁰ All these behaviors are certainly related to the particular CEF scheme of the Nd³⁺ ion, which can be easily modified by a magnetic field or changes in the composition.

Considering all this previous information, our system (NdNi_{1-x}Cu_x) provides a nice opportunity to investigate the evolution from a simple ferromagnetic structure in the Ni rich side to a more complex situation on the Cu rich one. In this way, our aim in the present paper is to shed some light on the Nd³⁺ magnetic ground state of this NdNi_{1-x}Cu_x series through an analysis of the magnetic properties (susceptibility, magnetization, resistivity) together with the determination of the magnetic structures obtained from neutron diffraction experiments, and then discuss the role of the main interactions governing these physical properties.

II. EXPERIMENTAL DETAILS

The NdNi_{1-x}Cu_x samples present intrinsic difficulties for crystallizing, especially close to the NdCu limit, because the melting process is not eutectic. We have paid special attention to finding the best preparation conditions for these compounds. These conditions (high melting temperatures and rapid quenching rates around 10³ °C/s) were obtained in an adequate arc furnace at the University of Savoie, France. We obtained polycrystalline samples with the FeB-type structure (Pnma space group) for the $x=0.4, 0.6, 0.8, 0.9,$ and 1.0 compositions. The samples were then annealed for 4 days at 450 °C; however, no improvement in the quality of the FeB diffraction patterns was found. The samples were homogeneous in composition, at least down to the micrometric scale, as deduced from the analysis with a scanning electron microscope. The crystallographic structures of the samples were checked by x-ray and neutron diffraction measurements.

The electrical resistivity between 1.9 and 300 K was measured by the ac four probe method, and the magnetization and the ac magnetic susceptibility were measured using a PPMS Quantum Design device at the Laboratory of Magnetism (Univ. de Cantabria, Spain). High field magnetization measurements were performed with a 23 T magnetometer at the Grenoble High Magnetic Field Laboratory. Neutron diffraction patterns down to 2 K were collected at the D1B diffractometer at the Institute Laue-Langevin, Grenoble, France, $\lambda=2.52$ Å being the wavelength used for these experiments. The analysis of crystallographic and magnetic structures were carried out by means of the Rietveld method using the program FULLPROF.¹¹

TABLE I. Crystallographic data of the NdNi_{1-x}Cu_x compounds obtained in the paramagnetic phase from data collected in D1B with a wavelength of 2.52 Å.

x	a (Å)	b (Å)	c (Å)	V (Å ³)	x (Nd)	z (Nd)	x (Ni/Cu)	z (Ni/Cu)	R_B (%)	T (K)
0.4	7.190(2)	4.401(1)	5.517(2)	174.9(3)	0.185(1)	0.143(4)	0.041(1)	0.634(3)	8.5	40
0.6	7.220(1)	4.440(1)	5.532(1)	177.3(1)	0.183(2)	0.142(3)	0.029(4)	0.615(2)	5.8	40
0.7	7.259(1)	4.478(1)	5.562(2)	180.8(2)	0.184(1)	0.134(2)	0.033(3)	0.623(1)	7.7	50
0.8	7.283(2)	4.506(2)	5.558(1)	182.4(3)	0.181(3)	0.122(2)	0.035(2)	0.620(2)	7.3	40
0.9	7.295(1)	4.529(1)	5.555(1)	183.5(1)	0.183(1)	0.122(3)	0.031(4)	0.616(1)	3.7	40
1.0	7.310(1)	4.564(1)	5.583(2)	186.3(2)	0.179(3)	0.130(4)	0.033(3)	0.615(2)	5.7	40

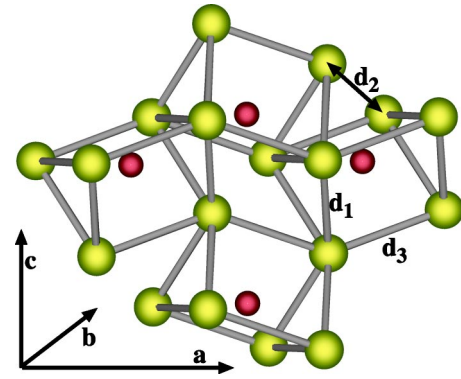


FIG. 1. Crystal structure of NdNi_{1-x}Cu_x ($x \geq 0.4$) with an orthorhombic FeB-type structure. The largest circles correspond to Nd³⁺ ions, while the smaller ones are Ni/Cu ions.

III. RESULTS

A. Crystallographic data

All the NdNi_{1-x}Cu_x ($x \geq 0.4$) studied compounds crystallize in the orthorhombic FeB-type structure. This structure is built up from trigonal prisms with the Nd³⁺ ions at the corners and the Ni/Cu ions randomly distributed at the center, as shown in Fig. 1. The refined crystallographic cell parameters and the atomic positions of Nd and Ni/Cu ions (respectively, located in two 4c sites with different x and z coordinates) obtained from the Rietveld analysis in the paramagnetic phase of these compounds are presented in Table I. The cell volume increases almost linearly with an increasing Cu content. The b cell parameter presents a larger variation (4%) than the a and c ones (only 1%). The Nd—Nd distances between the three first nearest neighbors (shown in Fig. 1, and named d_1, d_2, d_3) are represented as a function of the Cu content in Fig. 2. It is worth noting the relative change of the nearest neighbor distances. In fact, for $x=0.4$ the distances d_2 and d_3 are almost the same, but d_2 evolves towards the d_1 value when approaching $x=0.8$, which corresponds to the composition of the F-AF crossover. On the contrary, the Nd—Cu distances are almost unchanged throughout the series.

Very recent results have extended the stability domain of the FeB structure for $x \geq 0.25$, finding a new monoclinic Pm-type structure for NdNi_{0.825}Cu_{0.175}.¹² This kind of monoclinic structure was also found in the TbNi_{1-x}Cu_x (Ref. 13) and GdNi_{1-x}Cu_x (Ref. 2) series.

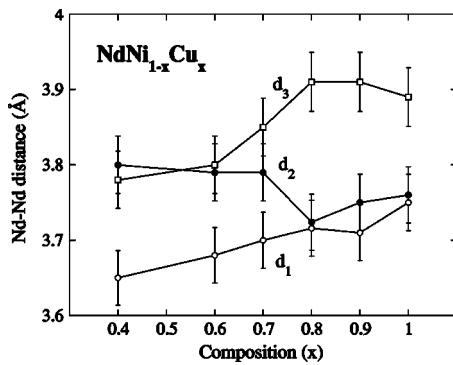


FIG. 2. Dependence of the first three Nd–Nd nearest neighbor distances with the Cu content in NdNi_{1-x}Cu_x.

B. Susceptibility and magnetization

The reciprocal paramagnetic susceptibility χ^{-1} of the studied NdNi_{1-x}Cu_x compounds is depicted in Fig. 3. Although all these compounds show a clear Curie-Weiss law for temperatures higher than 40 K (with a change of sign in the paramagnetic Curie temperature θ_p for $x \approx 0.8$; see inset of Fig. 3), the slopes of χ^{-1} are slightly different. This feature, previously observed in other R-Ni-based systems,¹⁴ is due to conduction band effects that lead to a modified Curie-Weiss law, $\chi = C(1 + \alpha)^2 / (T - \theta_p)$, where C is the Curie constant for the paramagnetic moment ($\mu_{eff} = 3.62 \mu_B$) of the Nd³⁺ free ion, and α is a phenomenological parameter describing polarization effects of the conduction band. The dependence of α with the Cu content is also presented in the inset of Fig. 3. This variation shows a sudden decrease around $x=0.8$, i.e., close to the above mentioned crossover from F to AF. This crossover is also shown in the temperature dependence of the M/H curves under an applied magnetic field of 2 kOe (see Fig. 4). The ordering temperatures in the ferromagnetic compounds, presented in Table II, are determined from the extrapolation of the magnetization curves when M/H tends to 0, and coincide with those obtained from the Arrott plot.

In the case of the $x=0.8$ compound, apart from the F transition detected at 27 K, a change of slope is observed at

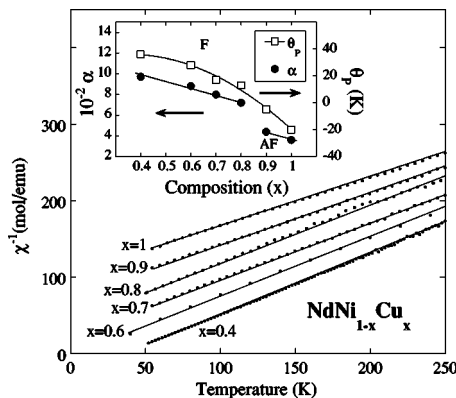


FIG. 3. Temperature dependence of the reciprocal paramagnetic susceptibility, χ^{-1} , of the NdNi_{1-x}Cu_x samples. The values are separated for the clarity of presentation. The inset shows the variation of α and θ_p with the Cu content (see the text).

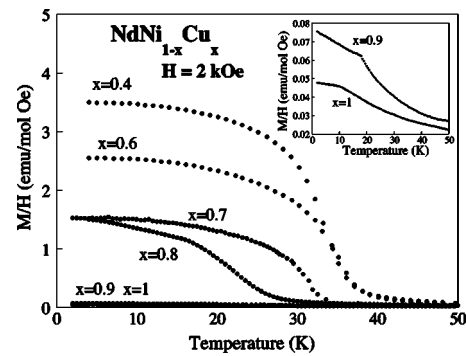


FIG. 4. Temperature dependence of M/H for NdNi_{1-x}Cu_x with an applied magnetic field of $H = 2$ kOe. The inset details the behavior of the AF compounds.

17 K, reminiscent of a supplementary antiferromagnetic behavior. The M/H values of the AF compounds $x=0.9$ and $x=1$ are one order of magnitude smaller than those of the F ones. From these curves, depicted in the inset of Fig. 4, we can determine the Néel temperatures at 18 K and 11 K for NdNi_{0.1}Cu_{0.9} and NdCu, respectively. However, we need the help of supplementary measurements performed with other techniques (resistivity or neutron diffraction) to detect the existence of other transitions, due to the very slight changes in the M/H curves in that temperature range.

In the F compounds, the magnetization measurements done after a zero field cooling (ZFC) and those obtained from field cooling (FC) are different (see Fig. 5). This behavior is attributed to the motion of narrow domain walls frozen by the strong magnetic anisotropy, as was also observed in other Rare Earth ferromagnetic compounds.¹⁵ The characteristic temperature T_W (defined as the inflection point of the ZFC variation) corresponds to the thermal energy necessary to move the domain wall under a magnetic field of 200 Oe. Similarly, the magnetization curves measured at 2 K up to 80 kOe indicate the existence of a threshold field H_W , needed in order to initiate the narrow wall shift (see Fig. 6). The value of H_W roughly decreases with increasing temperature. All these data are presented in Table II. The changes of T_W and H_W through the series for the different ferromagnetic compounds are a clear indication of the changes on the magnetocrystalline anisotropy.

The magnetization curves of the AF compounds (e.g., NdCu, presented in Fig. 6) show a soft transition centered around a critical field $H_C \approx 40$ kOe. A smooth hysteresis appears around that value when we decrease the applied magnetic field. Furthermore, the high magnetic field magnetization curves (up to 230 kOe) at 4 K for $x=0.7, 0.8, 0.9$, and 1.0 are presented in Fig. 7. They clearly show that the saturation is not reached even in such a high field. The saturation magnetization extrapolated at a zero field (M_0) for the ferromagnetic compounds is around $1.4 \mu_B$. Taking into account the magnetic structure (noncollinear ferromagnetic) we can estimate from these magnetization curves on polycrystals¹⁶ the value of the intrinsic Nd magnetic moment $\mu = 2M_0 \approx 2.8 \mu_B$, smaller than the Nd³⁺ free ion value ($3.27 \mu_B$). This reduction will be explained as a consequence of the CEF effects. The AF compounds are characterized by the absence

TABLE II. Magnetic parameters of the $\text{NdNi}_{1-x}\text{Cu}_x$ compounds, μ_{eff} being the effective paramagnetic moment and θ_p the paramagnetic Curie temperature obtained from the usual Curie-Weiss law $\chi=C/(T-\theta_p)$. For the ferromagnetic compositions, the critical temperature for the wall shift T_W was obtained at 200 Oe and the critical field for the wall shift (H_W) was obtained at 2 K. For the antiferromagnetic compositions, the metamagnetic transitions (H_C) were obtained at 2 K.

x	T_C (K)	T_N (K)	T_t (K)	$\mu_{\text{eff}}(\mu_B)$	θ_p (K)	T_W (K)	H_W (kOe)	H_C (kOe)
0.4	37.5	-	-	3.25(2)	36	12	2	-
0.6	37.0	-	-	3.30(2)	28	17	3	-
0.7	34.0	-	-	3.33(2)	17	22	6	-
0.8	27.0	-	17.0	3.36(2)	13	16	5	-
0.9	-	18.0	12.0	3.43(2)	-5	-	-	30
1.0	-	16.0	11.0	3.49(2)	-20	-	-	40

of clear-sharp metamagnetic transitions, but they exhibit quite smooth ones at certain critical field H_C , as explained before and reported in Table II. Furthermore, the magnitude of the magnetic field for achieving the saturation is larger in the AF compounds than in the F ones. This fact is not surprising because in AF compounds this saturation field depends on both the CEF anisotropy and the difference $J(\vec{q})-J(0)$, where $J(\vec{q})$ is the Fourier transform of the exchange interactions for the magnetic periodicity \vec{q} ,¹⁷ different from zero in the AF compounds. All these features are proof of the existence of a strong magnetocrystalline anisotropy in these $\text{NdNi}_{1-x}\text{Cu}_x$ materials. The main characteristics of the magnetic properties of these compounds are shown in Table II and suggest a very complex magnetic arrangement for the AF compounds.

C. Electrical resistivity

The temperature dependence of the electrical resistivity normalized to the value measured at room temperature is shown in Fig. 8 together with the temperature derivative of the normalized resistivity, in order to better locate the transition temperatures. The change in slope observed for the F compounds corresponds to the magnetic transitions detected by magnetization measurements. It is interesting to note that these changes are broader when the Cu content increases. For $x=0.9$ a slight change of slope, better defined in the resistivity derivative, is observed around $T_N=18$ K, while for $x=1$ a

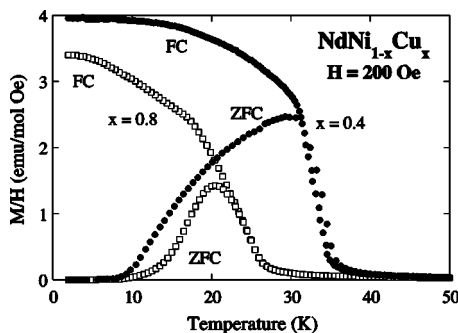


FIG. 5. Magnetization under a field of 200 Oe in field cooling (FC) and zero field cooling (ZFC) conditions for the $x=0.4$ and 0.8 compounds.

knee is found around 15 K. These transition temperatures, not well detected by magnetization measurements for the AF samples, will be confirmed later by neutron diffraction experiments in the next section. The brittle character of the samples means that the determination of the magnetic contribution, ρ_{mag} , to the electrical resistivity is not straightforward. However, following the procedure explained elsewhere,³ we have obtained the ρ_{mag} curves using as a non-magnetic reference the isostructural YNi compound for estimating the lattice contribution.

In Fig. 9 we present the temperature dependence of the magnetic contribution to the electrical resistivity below the ordering temperature. This contribution is related to the character of the magnetic structures. (Equal moment or amplitude modulated arrangements.) In particular, the low temperature variation of ρ_{mag} is faster for the AF samples than for the F ones. This feature, previously observed in RGa_2 (Ref. 18) and RNi_2Si_2 (Ref. 19), is related to entropy effects and indicates that the magnetic structures become more and more complex with the increase in Cu content, as we shall see in the neutron diffraction study.

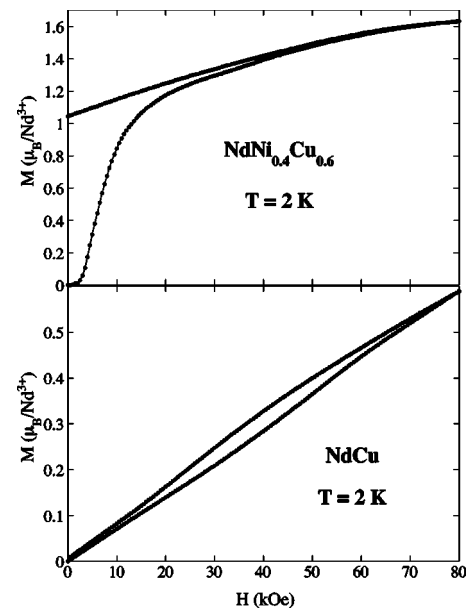


FIG. 6. Magnetization measurements at 2 K in $\text{NdNi}_{0.4}\text{Cu}_{0.6}$ and NdCu .

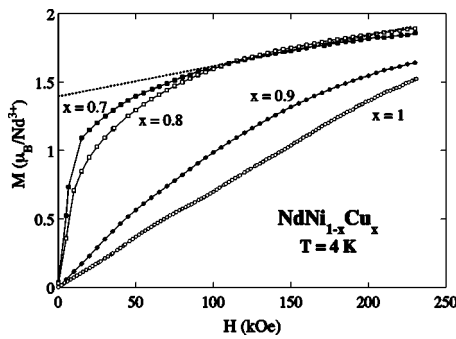


FIG. 7. High magnetic field magnetization measurements in selected NdNi_{1-x}Cu_x compositions ($x=0.7, 0.8, 0.9$ and 1.0).

In all of the samples ρ_{mag} keeps on increasing above T_C or T_N , reaching the saturation resistivity value around 200 K. This behavior of ρ_{mag} is due to CEF effects on the resistivity, and the temperature at which the saturation takes place provides an estimate of the magnitude of the total CEF splitting.²⁰ Thus, this total splitting seems to be roughly the same for all the studied NdNi_{1-x}Cu_x compounds.

D. Magnetic structures

The ferromagnetic compounds with $x=0.4, 0.6,$ and 0.7 exhibit almost identical magnetic diffraction patterns, thus indicating the same underlying magnetic structure. As an example of this magnetic contribution to the neutron diffraction, the difference pattern 2 K–40 K of NdNi_{0.4}Cu_{0.6} is dis-

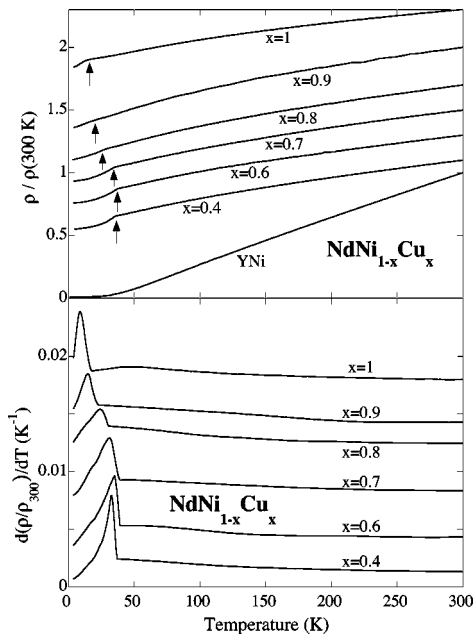


FIG. 8. Top: Temperature dependence of the electrical resistivity normalized to the value at 300 K in NdNi_{1-x}Cu_x compounds. The values are separated for clarity of comparison. The arrows indicate the ordering transition for each composition. Bottom: Temperature derivative of the normalized electrical resistivity, where the transition temperatures can be better seen. The values are also separated for clarity of comparison.

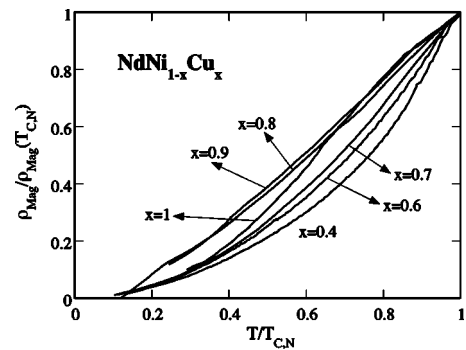


FIG. 9. Temperature dependence of the magnetic contribution to the electrical resistivity in NdNi_{1-x}Cu_x compounds normalized at the ordering temperature.

played in Fig. 10. The Rietveld analysis leads to a noncollinear ferromagnetic F_x-C_z mode (Bertaut's notation)²¹ with a $\vec{q}=0$ propagation vector. The value of the magnetic moment obtained from the refinement for these three compositions is around $2.6\mu_B$, in agreement with the value estimated from magnetization measurements.

A sketch of the magnetic arrangement corresponding to one of these compositions ($x=0.4$) is displayed in the inset of Fig. 10, as well as the temperature evolution of the magnetic moment value, defining a T_C of 37 K, in agreement with magnetization and resistivity measurements. It is worth noting that the angle of the magnetic moment with the **a** axis is temperature independent and its magnitude is close to 30°, showing that the anisotropy neither changes with temperature nor with composition in the F compounds. This type of magnetic structure is very common in orthorhombic FeB pseudoequatomic compounds.¹

The same type of ferromagnetic structure is found for $x=0.8$ in the temperature range $18\text{ K} < T < 27\text{ K}$. However, in this compound a low angle peak around $2\theta=7^\circ$ appears below 18 K and its intensity increases notoriously when the temperature is lowered (the inset of Fig. 11). This peak corresponds to a low temperature phase below T_C . As previously commented, a careful look at the magnetization mea-

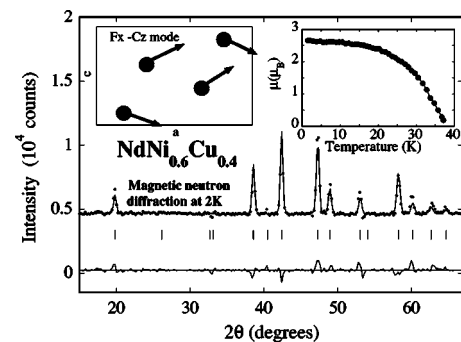


FIG. 10. Magnetic contribution at 2 K to the neutron diffraction pattern for NdNi_{0.6}Cu_{0.4}. It has been obtained by subtracting the paramagnetic pattern at 40 K. Points correspond to the experimental data while the line is the calculated pattern. Vertical ticks identify the magnetic reflections. The inset shows the Nd magnetic moment arrangement within the unit cell and the temperature dependence of the magnetic moment value.

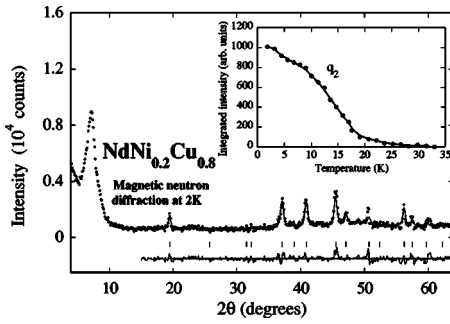


FIG. 11. Magnetic contribution at 2 K to the neutron diffraction pattern for $\text{NdNi}_{0.2}\text{Cu}_{0.8}$. It has been obtained by subtracting the paramagnetic pattern at 40 K. The inset shows the temperature dependence of the magnetic intensity of the low angle magnetic peak observed around $2\theta=7^\circ$ associated with \vec{q}_2 .

measurements (Fig. 4) shows a slight anomaly around this temperature (18 K). The low angle peak ($2\theta=7^\circ$) can be indexed with an incommensurate propagation vector \vec{q}_2 of modulus 0.28 \AA^{-1} . This propagation vector is associated with the appearance of an incommensurate AF arrangement of the magnetic moments. Furthermore, the full width at half maximum of this low angle peak (larger than those associated with the ferromagnetic structure, see Fig. 11) reflects a lack of magnetic homogeneity for this incommensurate arrangement, with important short-range spin correlations, indicating damage in the simple ferromagnetic structure. However, Rietveld refinements were not possible at low temperatures in this sample due to the absence of significant intensity in the peaks associated with the \vec{q}_2 propagation vector. At low temperatures, the full structure of this sample is similar to that proposed for $\text{CeNi}_{0.2}\text{Cu}_{0.8}$.²²

The magnetic patterns of the AF samples $x=0.9$ and 1.0 (see Figs. 12 and 13) present a large number of magnetic peaks at low temperatures, associated with the two propagation vectors needed to account for the magnetic contribution of these compounds. The analysis of the low-angle magnetic peak intensities of $\text{NdNi}_{0.1}\text{Cu}_{0.9}$ allows us to determine two different magnetic phases: the first one (\vec{q}_1) associated with the peak appearing at $2\theta=7.1^\circ$ below $T_N=18$ K and the second one (\vec{q}_2) related to the peak at $2\theta=9.1^\circ$ observed below $T_I=12$ K (see the inset of Fig. 12). While the 18 K transition

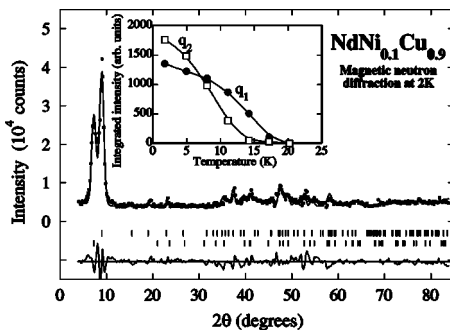


FIG. 12. A magnetic contribution at 2 K to the neutron diffraction pattern for $\text{NdNi}_{0.1}\text{Cu}_{0.9}$. It has been obtained by subtracting the paramagnetic pattern at 40 K. The inset shows the temperature dependence of the intensity of the peaks associated with \vec{q}_1 and \vec{q}_2 .

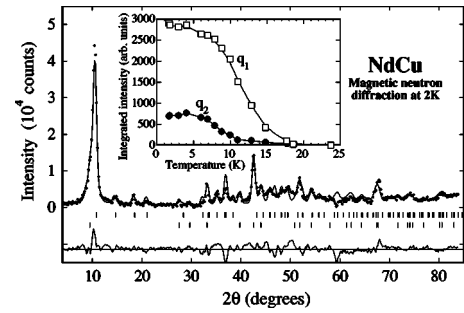


FIG. 13. Magnetic contribution at 2 K to the neutron diffraction pattern for NdCu . It has been obtained by subtracting the paramagnetic pattern at 40 K. The inset shows the temperature dependence of the intensity of the peaks associated with \vec{q}_1 and \vec{q}_2 .

was already found in magnetization and resistivity measurements, the 12 K one has been only shown by neutron diffraction. The magnetic pattern of $\text{NdNi}_{0.1}\text{Cu}_{0.9}$ at 2 K can be accounted for by the contribution of two coexisting helimagnetic phases: one of them with a propagation vector $\vec{q}_1=(0,0.24,0)$ and a $\mu=1.4 \mu_B$ magnetic moment within the \mathbf{xz} plane, and another one, appearing below 12 K, associated with a new independent propagation vector $\vec{q}_2=(0.3,0,0.28)$ but in this case with the magnetic moments lying in the \mathbf{xy} plane (see Table III). The proximity of $|\vec{q}_1|$ to the value obtained for the incommensurate magnetic structure found in $\text{NdNi}_{0.2}\text{Cu}_{0.8}$ might indicate that the latter could be a short-range order precursor of the magnetic structure already well established in the $\text{NdNi}_{0.1}\text{Cu}_{0.9}$ sample.

The magnetic Rietveld refinement gives a reasonable accuracy ($R_B=17\%$), when both magnetic phases contribute at 50%. It is worth noting that we cannot really distinguish between an amplitude modulated and a helimagnetic structure below T_N using neutron diffraction on powdered samples. However, when the temperature is lowered, the amplitude modulated magnetic structures cannot be stable down to 0 K due to the Kramers character of the Nd^{3+} ions, and usually transform (i) either into an AF equal magnetic moment structure through a magnetic phase transition with a

TABLE III. A summary of the magnetic structure data: the propagation vector \vec{q} (in some of these compounds below a determined temperature two propagation vectors are needed to describe the magnetic structure), the structure type, the magnetic moment value; and the Bragg factor of the magnetic refinement.

x	\vec{q}	Structure type	$\mu(\mu_B)$ at 2 K	$R_B(\%)$
0.4	0	Fx-Cz	2.6	14
0.6	0	Fx-Cz	2.7	11
0.7	0	Fx-Cz	2.6	12
0.8	$\vec{q}_1=0$ $q_2=0.28 \text{ \AA}^{-1}$	Ferro ?	1.6 ?	15
0.9	$\vec{q}_1=(0,0.24,0)$ $\vec{q}_2=(0.3,0,0.28)$	Heli-xy Heli-xz	1.4 2.5	17
1.0	$\vec{q}_1=(0.37,0,0.33)$ $\vec{q}_2=(1/2,0,0)$	Heli-xyz AF-xz	2.0 1.8	17

change of propagation vector; or (ii) into an antiphase structure without a defined magnetic transition, keeping the same propagation vector but giving rise to the appearance of higher order harmonics of the propagation vector.¹ Neither of them seems to be the situation of $x=0.9$ (and also 1.0; see below). Then, the helimagnetic structure seems to be the most plausible choice.

Finally, as in the previous case, the neutron diffraction study on NdCu allows us to determine precisely an ordering temperature of $T_N=16$ K. It orders with a helimagnetic structure just below T_N with a propagation vector $\vec{q}_1=(0.37,0,0.33)$ (close to that found above in $x=0.9$ at low temperatures) and with magnetic moment components in the three spatial directions. At temperatures below $T_I=11$ K the observed additional magnetic contribution (see the inset of Fig. 13) can be indexed with a propagation vector $\vec{q}_2=(1/2,0,0)$ and the magnetic moments in the \mathbf{xz} plane. The magnetic structure associated with this propagation vector was also found in CeCu.²² Although helimagnetic structures are forbidden by group theory under orthorhombic symmetry,²³ it must be stressed that this theory is applied in compounds with a well defined symmetry. The substitution of Ni by Cu leads to a failure on the local symmetries introducing additional degeneracy, which could allow such helimagnetic structures. Examples of such magnetic structures in orthorhombic substitutional compounds can be found elsewhere.^{3,24} The main characteristics of the magnetic structure analysis are presented in Table III.

From the present results it is clear that a considerable magnetic complexity appears in the compounds with a larger Cu content, leading to incommensurate structures that are characterized by noninteger propagation vectors. The value of these propagation vectors is very sensitive to composition and then, slight inhomogeneities in the samples (not detected by x-ray or nuclear neutron diffraction) induce a magnetic phase segregation that is visible via magnetic diffraction. A similar phenomenology has recently been described in the TbPt_{1-x}Cu_x series.²⁵

IV. DISCUSSION

In this paper an extensive study of the magnetism in the NdNi_{1-x}Cu_x series is reported, including magnetic structures, resistivity, magnetic susceptibility, and the magnetization process. The main results are presented in Tables I–III. The use of complementary techniques allows a more realistic magnetic characterization, because sometimes the information obtained from only one technique is not enough to properly determine the magnetic properties. In this sense, different magnetic transitions have been shown in the AF compounds. Their Néel or transition temperatures have been determined as well as their temperature range of stability. Neutron diffraction was particularly important to ascertain the coexistence of phases arising from the complex magnetic behavior of these materials.

The first point to be discussed is related to the magnetic structures in these samples. For the F compounds ($x<0.8$) quite a simple noncollinear F_x-C_z mode is found, while the AF compounds at low temperatures are described by two

different propagation vectors with considerably complex magnetic arrangements.

Taking into account the substitutional disorder Ni and Cu in the same crystallographic site through the NdNi_{1-x}Cu_x series, the most complicated magnetic behavior could be interpreted as a consequence of the presence of microscopic magnetic inhomogeneities or zones with a slightly different Cu/Ni composition, as already pointed out in diluted TbNiAl compounds^{26,27} and TbPt_{1-x}Cu_x.²⁵ However, two propagation vectors have also been found in pure NdCu, making it difficult to assume this hypothesis as the only explanation for the observed behavior. As mentioned in the Introduction, NdCu₂ also presents a complicated situation: several single crystal studies^{28,29} point out the coexistence of different AF phases, also determined by neutron diffraction in polycrystalline samples.⁹ On the other hand, the Néel temperature of NdCu₂ is around 7 K. In our neutron diffraction study on NdCu, the magnetic peaks of the two found phases appear at 16 and 11 K, respectively (see Fig. 13), thereby discarding the presence of NdCu₂ as the cause of these transitions. So, we need to assume that this complex behavior is due to an intrinsic characteristic of these compounds.

In particular, this behavior seems to be related to the shape of the Fourier transform of the exchange interactions $J(\vec{q})$ that has to be minimized for the \vec{q} value of the stable magnetic structure. From the present neutron diffraction results it turns out that $J(\vec{q})$ reaches minima in several positions out of the principal symmetry points in the \vec{q} space. This situation resembles the “nesting effect” discussed by Dzyaloshinskii for rare earth metals.³⁰ The nesting hypothesis that links the existence of incommensurate magnetic structures with the shape of the Fermi surface has raised a renewed interest due to the observation of webbing Fermi surfaces in Y³¹ and YGd compounds,³² recent local spin density calculations³³ or the discussion about the magnetic structures in Tb_{1-x}Tm_x alloys.³⁴ This effect has also been invoked to describe the origin of nonconventional superconductivity in RNi₂B₂C (R=Y, Lu).³⁵

There is a direct correlation between \vec{q} and the shape of the Fermi surface that plays a crucial role in the existence of these complicated structures. In fact, these structures have been found in many orthorhombic²⁴ or hexagonal³⁴ compounds, and, generally, the Fermi surface shape is very sensitive to any structural or electronic change. In particular, in our NdNi_{1-x}Cu_x series, small variations in both the number of conduction electrons or the crystalline lattice parameters strongly affect the Fermi surface shape and different \vec{q} values can be found. Although studies on single crystals as well as band structure calculations are needed to determine the actual shape of the Fermi surface and its relation with \vec{q} , we have many indications on their criticality close to NdCu. In this sense, the crystallographic study presented before shows that the first and second neighbor Nd–Nd distances are quite similar on the Cu-rich side, and, in consequence, the exchange coupling constant associated with these neighbors could be quite competitive in determining the magnetic ordering for the AF compounds. Furthermore, the modifications in the J_{ij} coupling constant are demonstrated by the susceptibility measurements, because both $\theta_p=J(0)=\sum_{j\neq i}J_{ij}$ and the α coefficient (related to the Curie-Weiss law slope)

change significantly close to the $x=0.8$ concentration when crossing from F to AF ordering in $\text{NdNi}_{1-x}\text{Cu}_x$ (see Sec. III B). It is worth mentioning that the α parameter is directly related to the density of states at the Fermi level; then, the susceptibility measurements indicate a decrease of this density of states when approaching the AF limit, in agreement with the conclusions obtained from thermopower measurements.³⁶ All these results support recent models³⁷ that point out the importance of the density of states at the Fermi level in establishing a ferro- or antiferromagnetic type of ordering.

In this study of the $\text{NdNi}_{1-x}\text{Cu}_x$ series, no traces of spin-glass-like behavior have been found. The χ_{ac} measurements do not present any shift in the maximum at T_C with the frequency or the applied magnetic field, quite the contrary to what happens in the parallel $\text{CeNi}_{1-x}\text{Cu}_x$ series.⁴ This is a fine confirmation of the need for strong $4f$ -conduction band hybridization (Kondo interactions) to establish the spin-glass phase in these kinds of substitutional compounds.

The magnetic contribution to the electrical resistivity below the ordering temperature is also quite sensitive to the magnetic evolution of the system. For the ferromagnetic compounds, ρ_{mag} exhibits a rapid variation close to T_C , while for the AF ones, a smooth variation appears. As previously observed and discussed in RGa_2 (Ref. 18) and RNi_2Si_2 (Ref. 19) compounds, this temperature dependence is quite closely related to thermal effects on the thermodynamical entropy associated with the magnetic system. Then, a clear link between the magnetic contribution to the electrical resistivity and the entropy due to the $4f$ electrons in $\text{NdNi}_{1-x}\text{Cu}_x$ can be

established, showing that with the dilution of Cu, the magnetic structures become more complex, leading to less defined magnetization processes.

The last comment to be made focuses on the fact that the magnetic moments seem to behave quite randomly when considering their direction through the $\text{NdNi}_{1-x}\text{Cu}_x$ series. The strong magnetocrystalline anisotropy pointed out by the magnetization measurements determine the direction of the magnetic moments in the magnetic structure. Indeed, for the F compounds the \mathbf{xz} plane is the easy magnetization plane, while for the AF compounds the \mathbf{xy} plane is the easy one for some of the propagation vectors involved in the description of the magnetic structures at low temperatures. This fact supports the relevance of CEF terms of higher order than two, probably with two very close low-lying levels, and possibly the presence of anisotropic exchange interactions in the Hamiltonian.

In order to elucidate the different aspects commented upon and the role played by the exchange and CEF interactions, an extensive study devoted to determining the CEF level scheme is under preparation and will be presented in a subsequent paper.

ACKNOWLEDGMENTS

This work was supported by the Spanish CICYT, Grant No. MAT2002-04178-C04. The support of Luis Echeandia is gratefully acknowledged. We are very much indebted to G. Chouteau for his help in the high field magnetization measurements.

-
- ¹D. Gignoux and D. Schmitt, in *Handbook of Magnetic Materials*, edited by K. H. J. Buschow (Elsevier Science, City, 1997), Vol. 10, p. 239.
- ²D. Gignoux and J. C. Gómez Sal, *J. Magn. Magn. Mater.* **1**, 203 (1976).
- ³J. A. Blanco, J. C. Gómez Sal, J. Rodríguez Fernández, D. Gignoux, D. Schmitt, and J. Rodríguez-Carvajal, *J. Phys.: Condens. Matter* **4**, 8233 (1992).
- ⁴J. García Soldevilla, J. C. Gómez Sal, J. A. Blanco, J. I. Espeso, and J. Rodríguez Fernández, *Phys. Rev. B* **61**, 6821 (2000).
- ⁵J. García Soldevilla, J. C. Gómez Sal, J. Rodríguez Fernández, J. I. Espeso, and M. A. Argüelles, *J. Magn. Magn. Mater.* **186**, 49 (1998).
- ⁶J. García Soldevilla, J. I. Espeso, J. Rodríguez Fernández, J. C. Gómez Sal, J. A. Blanco, P. Galez, and D. Paccard, *J. Magn. Magn. Mater.* **157–158**, 624 (1996).
- ⁷J. C. Gómez Sal, J. I. Espeso, J. Rodríguez Fernández, N. Marciano, and J. A. Blanco, *J. Magn. Magn. Mater.* **242–245**, 125 (2002).
- ⁸E. M. Forgan, E. P. Gibbons, K. A. McEwen, and D. Fort, *Phys. Rev. Lett.* **62**, 470 (1989).
- ⁹R. R. Arons, M. Loewenhaupt, Th. Reif, and E. Gratz, *J. Phys.: Condens. Matter* **6**, 6789 (1994).
- ¹⁰J. García Soldevilla, J. I. Espeso, J. Rodríguez Fernández, J. C. Gómez Sal, J. A. Blanco, and M. T. Fernández Díaz, *J. Magn. Magn. Mater.* **196–197**, 898 (1999).
- ¹¹J. Rodríguez-Carvajal, *Physica B* **192**, 55 (1993).
- ¹²D. Paccard, J. Allemand, J. M. Moreau, J. C. Gómez Sal, J. Rodríguez Fernández, J. I. Espeso, and J. A. Blanco, *J. Alloys Compd.* **381**, 63 (2004).
- ¹³R. Lemaire and D. Paccard, *J. Less-Common Met.* **21**, 403 (1970).
- ¹⁴V. M. T. S. Barthém, D. Gignoux, A. Nait-Saada, D. Schmitt, and G. Creuzet, *Phys. Rev. B* **37**, 1733 (1988).
- ¹⁵B. Barbara, *J. Phys. (France)* **34**, 1039 (1973).
- ¹⁶A. Castets, D. Gignoux, J. C. Gómez Sal, and E. Roudaut, *Solid State Commun.* **44**, 1329 (1982).
- ¹⁷T. Nagayima, K. Nagota, and Y. Kitano, *Prog. Theor. Phys.* **27**, 1253 (1962).
- ¹⁸J. A. Blanco, D. Gignoux, J. C. Gómez Sal, J. Rodríguez Fernández, and D. Schmitt, *J. Magn. Magn. Mater.* **104–107**, 1285 (1992).
- ¹⁹J. M. Barandiarán, D. Gignoux, D. Schmitt, J. C. Gómez Sal, and J. Rodríguez Fernández, *J. Magn. Magn. Mater.* **69**, 61 (1987).
- ²⁰V. U. S. Rao and W. E. Wallace, *Phys. Rev. B* **2**, 4613 (1970).
- ²¹E. F. Bertaut, *Acta Crystallogr., Sect. A: Cryst. Phys., Diffr., Theor. Gen. Crystallogr.* **24**, 217 (1968).
- ²²J. I. Espeso, J. García Soldevilla, J. A. Blanco, J. Rodríguez Fernández, J. C. Gómez Sal, and M. T. Fernández Díaz, *Eur. Phys. J. B* **18**, 625 (2000).

- ²³J. Rossat-Mignod, in *Neutron Scattering in Condensed Matter Research*, edited by K. Sköld and D. L. Price (Academic Press, New York, 1986), Chap. 20.
- ²⁴A. Szytula and J. Leciejewicz, in *Handbook on the Physics and Chemistry of Rare Earths*, edited by K. A. Gschneidner and L. Eyring (North-Holland, New York, 1989), Vol. 12, p. 133 and references therein.
- ²⁵A. Señas, J. Rodríguez Fernández, J. C. Gómez Sal, J. Campo, and J. André, *Physica B* **350**, 115 (2004).
- ²⁶G. Ehlers, D. Ahlert, C. Ritter, W. Miekeley, and H. Maletta, *Europhys. Lett.* **37**, 269 (1997).
- ²⁷G. Ehlers, C. Ritter, A. Krutjakow, W. Miekeley, N. Stüßer, Th. Zeiske, and H. Maletta, *Phys. Rev. B* **59**, 8821 (1999).
- ²⁸P. Svoboda, M. Divis, A. V. Andreev, N. V. Baranov, M. I. Bartashevich, and P. E. Markin, *J. Magn. Magn. Mater.* **104–107**, 1329 (1992).
- ²⁹M. Ellerby, K. A. McEwen, M. de Podesta, M. Rotter, and E. Gratz, *J. Phys.: Condens. Matter* **7**, 1897 (1995).
- ³⁰I. E. Dzyaloshinskii, *Sov. Phys. JETP* **20**, 223 (1965).
- ³¹S. B. Dugdale, H. M. Fretwell, and M. A. Alam, *Phys. Rev. Lett.* **79**, 941 (1997).
- ³²J. A. Duffy, S. B. Dugdale, J. E. McCarthy, M. A. Alam, M. J. Cooper, S. B. Palmer, and T. Jarlborg, *Phys. Rev. B* **61**, 14331 (2000).
- ³³L. Nordström and A. Mavromaras, *Europhys. Lett.* **49**, 775 (2000).
- ³⁴A. V. Andrianov, A. S. Il'iushin, D. I. Kosarev, V. S. Zaslavov, and B. Lebech, *J. Magn. Magn. Mater.* **251**, 25 (2002).
- ³⁵P. Martínez-Samper, H. Suderow, S. Vieira, J. P. Brison, N. Luchier, P. Lejay, and P. C. Canfield, *Phys. Rev. B* **67**, 014526 (2003).
- ³⁶J. Fontcuberta, A. Seffar, A. Hernando, J. C. Gómez Sal, and J. M. Rojo, *J. Appl. Phys.* **81**, 3887 (1997).
- ³⁷A. Hernando, J. M. Rojo, J. C. Gómez Sal, and J. M. Novo, *J. Appl. Phys.* **79**, 4815 (1996).